

## THE BULK LORENTZ FACTORS OF FERMI-LAT GRBS

XIAO-HONG ZHAO<sup>1,4</sup>, ZHUO LI<sup>2,3</sup>, JIN-MING BAI<sup>1,4</sup>*Draft version February 19, 2019*

## ABSTRACT

The Lorentz factor (LF) of gamma-ray burst (GRB) ejecta may be constrained by observations of high-energy (HE) spectral attenuation. The recent Fermi-LAT observations of prompt GeV emission from several bright GRBs have led to conclusions of unexpectedly large LFs,  $\Gamma > 10^3$ . Here we revisit this problem with two main concerns. (1) With one-zone assumption where all photons are assumed to be generated in the same region (radius) and time, we *self-consistently* calculate the  $\gamma\gamma$  optical depth by adopting a target photon spectrum with HE cutoff. We find that this might be important when the GRB LF is below a few hundreds. (2) Recent Fermi-LAT observations suggest that the bulk MeV-range and HE ( $\gtrsim 100$  MeV) emission may arise from different regions. We then consider a two-zone case where HE emission is generated in large radii and mainly attenuated by prompt MeV-range emission generated at small radii. We find that the attenuated HE spectrum does not show an exponential spectral cutoff but a slight steepening. This suggests that there may be no abrupt cutoff due to  $\gamma\gamma$  attenuation if relaxing the one-zone assumption. By studying the spectra of three bright Fermi-LAT GRBs 080916C, 090510 and 090902B, we show that a bulk LF of  $300 \lesssim \Gamma \lesssim 600$  can be consistent with observations.

*Subject headings:* gamma ray: bursts — gamma ray: observations

## 1. INTRODUCTION

Relativistic expansion is a key property of gamma-ray bursts (GRBs), and has been confirmed by measurements of radio afterglow sizes, for examples, the indirect estimation by radio scintillation in GRB 970508 (Waxman et al. 1998) and direct imaging of nearby GRB 030329 (Taylor et al. 2004). These observations revealed mildly relativistic GRB ejecta,  $\Gamma \sim$  a few, in the radio afterglow phase. However, it is well believed that GRB ejecta are ultra-relativistic in the beginning—this is required to solve the so-called "compactness problem" (e.g., Piran 1999). The compact GRB source, suggested by the rapid variabilities in MeV light curves, and the huge luminosity suggest hot, optically thick GRB sources, which is in conflict with the nonthermal and hard GRB spectra. Relativistic expansion of the emission region is introduced to solve this problem. In order for the  $\sim 100$  MeV photons, as detected by EGRET in several GRBs, to escape from the emission region, avoiding  $\gamma\gamma$  attenuation, the bulk Lorentz factor (LF) of the emission region is required to be extremely large,  $\Gamma \gtrsim 10^2$  (e.g., Lithwick & Sari 2001; Krolik & Pier 1991; Fenimore et al. 1993; Woods & Loeb 1995; Baring & Harding 1997). Recently, the powerful Fermi satellite reveals in much more detail the high-energy (HE) emission from GRBs. Several bright GRBs are reported to show time-integrated spectra extending up to GeV or even tens GeV, without any signs of spectral cutoff. Assuming the  $\gamma\gamma$  optical depth for these HE photons are below unity, these observations have led to even larger bulk LFs,  $\Gamma > 10^3$  (Abdo et al. 2009a,b,c). This is putting the theoretical problem of relativistic jet formation to extremes.

In the previous constraints two assumptions are usually

taken. First, all photons, from low to high energy, are produced in the same region and the same time. This "one-zone" assumption is not solid, as Fermi observations actually revealed that: the onset of HE emission is delayed relative to MeV emission (e.g., Abdo et al. 2009a,b,c); the HE emission lasts longer than MeV emission (e.g., Abdo et al. 2009a,b,c); the bulk emission shifts toward later time as the photon energy increases (Abdo et al. 2009a) and the shift is longer than the variability times in MeV light curves, as pointed out by (Li 2010); some GRBs obviously show distinct HE components with different temporal behaviors (Abdo et al. 2009b,c). All these features may imply that different energy photons are produced in different regions.

In particular, the bulk  $> 100$  MeV emission in GRB 080916C shows  $\sim 1$  s shifting relative to MeV emission, which is much longer than the MeV variability time,  $< 100$  ms as revealed by INTEGRAL (Greiner et al. 2009), strongly implying that  $> 100$  MeV emission is produced in a region of much larger radii than MeV emission's (Li 2010). As pointed out by Li & Waxman (2008), within the framework of internal shock model, the internal collisions at small radii, which would produce the prompt MeV emission, are expected to lead to "residual" collisions at much larger radii, which would produce low-frequency emission. The electrons accelerated by residual collisions at larger radii inverse-Compton scattering the MeV photons and/or double scattering the low-frequency photons could produce HE emission (Li 2010; Zhao et al. 2010). In this case, MeV and HE photons are produced in different regions. In the comoving frame of HE emission region, the MeV photons would be collimated other than isotropic, thus the  $\gamma\gamma$  absorption is angular dependent.

Second, the target photon spectrum is assumed to be extending to infinity. As pointed out by Li (2010), the calculation of  $\gamma\gamma$  optical depth taking such a target photon filed is obviously not self-consistent, because the HE spectral end should be cut off due to absorption considered in the calculation.

In this paper, we revisit the problem of GRB LF constraint

<sup>1</sup> National Astronomical Observatories/Yunnan Observatory, Chinese Academy of Sciences, P.O. Box 110, 650011 Kunming, China; zhaohx@ynao.ac.cn

<sup>2</sup> Department of Astronomy, Peking University, Beijing 100871, China

<sup>3</sup> Kavli Institute for Astronomy and Astrophysics, Peking University, Beijing 100871, China

<sup>4</sup> Key Laboratory for the Structure and Evolution of Celestial Bodies, Chinese Academy of Sciences, P.O. Box 110, 650011 Kunming, China

by modifying the above mentioned two assumptions. We consider in §2 a one-zone case where the  $\gamma\gamma$  optical depth is calculated *self-consistently* by assuming a truncated target spectrum, then we consider in §3 a simple two-zone case with anisotropic effect on  $\gamma\gamma$  optical depth taken into account. In §4 we studied the spectra of the three bright Fermi-LAT GRBs and constrain their LFs. §5 is discussion and conclusions. In the following we assume the concordance universe model with  $(\Omega_m, \Omega_\Lambda) = (0.27, 0.73)$  and  $H_0 = 71 \text{ km s}^{-1} \text{ Mpc}^{-1}$ .

## 2. ONE-ZONE CASE

Consider a GRB ejecta with bulk LF  $\Gamma$  and radius  $R$ . Assume the photons in the comoving frame of the ejecta is isotropic, with photon number density per photon energy  $dn'/d\epsilon'$ . Hereafter, unless specified otherwise, quantities with prime denote the comoving frame, and non-primed ones denote the frame of observer on the Earth.

In the (comoving-frame) dynamical time  $R/\Gamma c$ , a photon travels a path of  $R/\Gamma$ . For a photon of energy  $\epsilon' = \epsilon(1+z)/\Gamma$  (with  $z$  the GRB redshift), the optical depth due to  $\gamma\gamma$  collisions during a dynamical time is given by (Gould & Schröder 1967)

$$\tau(\epsilon') = \frac{R}{2\Gamma} \int_{m_e^2 c^4 / \epsilon'}^{\epsilon'_{\max}} \frac{dn'}{d\epsilon'} d\epsilon' \int_{-1}^1 (1-\mu') \sigma(E) d\mu', \quad (1)$$

where  $\mu' = \cos\theta'$  and  $\theta'$  is the angle between the colliding photon pair. The cross section is given by

$$\sigma(E) = \frac{3\sigma_T}{16} (1-\beta_e^2) \left[ (3-\beta_e^4) \ln \frac{1+\beta_e}{1-\beta_e} - 2\beta_e(2-\beta_e^2) \right] \quad (2)$$

where  $\beta_e = \sqrt{1-(m_e c^2/E)^2}$  and  $E = \sqrt{\epsilon' \epsilon' (1-\mu')/2}$  are the velocity and energy, respectively, of the generated electron in the center of momentum frame of the collision. The radius  $R$  of the emission region can be related to the angular spreading time  $\delta t_{\text{ang}}$ , due to geometry effect, by  $R = 2\Gamma^2 c \delta t_{\text{ang}} / (1+z)$ . As the angular spreading time is related to the observed variability time  $\delta t$  by  $\delta t_{\text{ang}} = \delta t$ , we have

$$R = 2\Gamma^2 c \frac{\delta t}{1+z}. \quad (3)$$

For a GRB with the observed photon number per unit time per unit photon energy per unit detector area, denoted by  $N(\epsilon)$ , the photon number density per unit photon energy in the comoving frame can be given by

$$\frac{dn'}{d\epsilon'} = \left( \frac{d_L}{R} \right)^2 \frac{N(\epsilon)}{c(1+z)^2}, \quad (4)$$

where  $d_L$  is the GRB luminosity distance, and  $\epsilon = \Gamma \epsilon' / (1+z)$ .

It is important to note a difference from the previous works. In eq. (1) we did not take the upper limit of the integration to be infinity but a certain photon energy  $\epsilon'_{\max}$ , because the HE tail is expected to be cut off due to  $\gamma\gamma$  absorption. The cutoff energy is just where  $\tau(\epsilon'_{\max}) = 1$  happens. To self-consistently solve out the cutoff energy  $\epsilon_{\max} = \Gamma \epsilon'_{\max} / (1+z)$  for given  $\Gamma$ , we need to take the upper limit of the integration to be  $\epsilon'_{\max}$ , and solve  $\tau(\epsilon'_{\max}) = 1$  using eqs. (1-4) and observed GRB spectrum  $N(\epsilon)$ .

It is well known that the GRB spectrum can be fit by the

Band function (Band et al. 1993)

$$N(\epsilon) = \begin{cases} A \left( \frac{\epsilon}{100 \text{ keV}} \right)^\alpha \exp \left[ -\frac{\epsilon(2+\alpha)}{\epsilon_p} \right] & \epsilon < \epsilon_c \\ A \left[ \frac{(\alpha-\beta)\epsilon_p}{(2+\alpha)100 \text{ keV}} \right]^{(\alpha-\beta)} \exp(\beta-\alpha) \left( \frac{\epsilon}{100 \text{ keV}} \right)^\beta & \epsilon > \epsilon_c \end{cases}, \quad (5)$$

where  $\epsilon_c = \epsilon_p(\alpha-\beta)/(2+\alpha)$ , and  $A$ ,  $\alpha$ ,  $\beta$  and  $\epsilon_p$  are the normalized coefficient, low-energy slope, HE slope and the  $\nu F_\nu$  peak energy, respectively. In some Fermi-LAT GRBs an extra spectral component beyond the Band-function is claimed to exist, especially in HE end (Abdo et al. 2009b,c). This extra component can be described as a power law,

$$N(\epsilon) = A_{\text{PL}} \left( \frac{\epsilon}{1 \text{ GeV}} \right)^{\beta_{\text{PL}}}, \quad (6)$$

with  $A_{\text{PL}}$  the normalization at 1 GeV and  $\beta_{\text{PL}}$  the spectral index.

It is helpful to solve out the  $\Gamma - \epsilon_{\max}$  relation with some approximations first. Typically the HE,  $\gtrsim 100$  MeV, photons mainly interact with photons above the peak energy. Let us approximate the target photon distribution as a single power law  $N(\epsilon) = N_0 \epsilon^{-s}$  in the following analytical derivation.

In eq. (1), usually the upper limit of the first integral is taken to be  $\infty$ . This is valid for  $\epsilon_{\max} \gg \Gamma^2 m_e^2 c^4 / [\epsilon_{\max}(1+z)^2]$  and the spectrum slope  $s > 1$ . In this case, using  $\delta$ -approximation for the cross section at target photon energy above the threshold,  $\sigma \approx (3/16)\sigma_T$ ,  $\tau(\epsilon_{\max}) = 1$  can be solved to give  $\Gamma$  as function of  $\epsilon_{\max}$ ,

$$\Gamma \propto \epsilon_{\max}^{\frac{1+s}{2(s-1)}}. \quad (7)$$

However, when  $\epsilon_{\max} \gtrsim \Gamma^2 m_e^2 c^4 / [\epsilon_{\max}(1+z)^2]$ , i.e., the energy of annihilated photons is compared with that of target photons, the upper limit cannot be taken as  $\infty$  any more. In the case,  $\Gamma$  is given by (Li 2010)

$$\Gamma \approx \frac{\epsilon_{\max}}{m_e c^2} (1+z). \quad (8)$$

Next we carry numerical calculation to solve out  $\tau(\epsilon_{\max}) = 1$ . For the observations, we take the three bright Fermi-LAT GRBs 080916C, 090510 and 090902B, and consider the same time intervals in the GRBs where the LFs have been constrained by Abdo et al. (2009a,b,c). The properties of spectra and flux for these GRBs are shown in Table 1. The calculated results are given in Fig 1, where we compare the results of self-consistent calculation and previous method using a target photon spectrum without HE cutoff. We see that the results deviate each other for  $\epsilon_{\max} \lesssim 100$  MeV or  $\Gamma \lesssim$  a few hundreds. But in the cases of these three GRBs, the LF constraints using upper limit of infinity are valid.

## 3. TWO-ZONE CASE

As discussed in the introduction, the Fermi-LAT observations hint that there may be different emission regions of different radii in GRB prompt emission. As the HE delay of onset and the shifting of the bulk HE emission are in seconds scale, whereas the MeV-range variability times, reflecting the dynamical time of the MeV emission region, are in tens of ms scale, the MeV emission regions have much smaller, by orders of magnitude, size (radius) than that of HE emission regions.

Consider that the ejecta expand to radius  $R$  where HE emission is being produced. The photons that are emitted in much smaller radii and just arrive at radius  $R$  should be produced by

TABLE 1  
THE PARAMETERS OF THREE BRIGHT LAT-GRBs

GRB name	Time interval (s)	$\epsilon_p$ (keV)	$\alpha$	$\beta$	$A$ ( $\text{cm}^{-2}\text{s}^{-1}\text{keV}^{-1}$ )	$\beta_{\text{PL}}$	$A_{\text{PL}}$ ( $\text{cm}^{-2}\text{s}^{-1}\text{keV}^{-1}$ )	$z$	$\delta t$ (ms)	$\epsilon_{\text{highest}}$ (GeV)
GRB 080916C	3.58-7.68	1170	-1.02	-2.21	0.035	—	—	4.35	100 <sup>a</sup>	3
GRB 090510	0.8-0.9	1894	-0.86	-3.09	0.028	-1.54	$6.439 \times 10^{-9}$	0.903	12	30.5
GRB 090902B	9.6-13	821	-0.26	-5.0	0.082	-1.98	$4.3 \times 10^{-10}$ <sup>b</sup>	1.822	53	11.2

NOTE. — References: a: Greiner et al. (2009); b: private communication with Francesco de Palma; and the other parameters are taken from Abdo et al. (2009a,b,c).

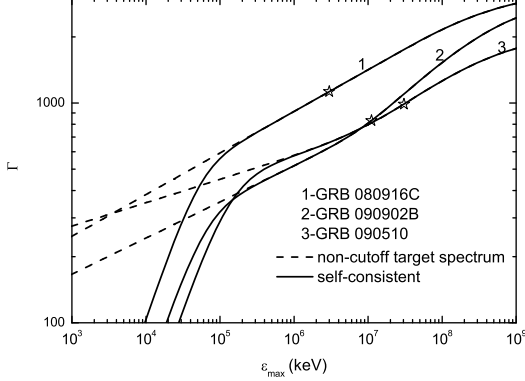


FIG. 1.— The  $\epsilon_{\text{max}} - \Gamma$  relation in the one-zone case and for the three bright GRBs. The adopted parameters of the GRBs are shown in Table 1. As marked in the plot, the dash lines correspond to results using target photon without spectral cutoff, while the solid lines correspond to our *self-consistent* calculations using truncated target photon spectra. The stars denote the observed highest energy of photons in the relevant time intervals.

those ejecta released from the central engine with a time delay of  $t_d = R(1+z)/2\Gamma^2 c$ . If  $t_d \gg \delta t$  then  $t_d$  is also the observed delayed time scale of the HE emission. Thus, once we observed a time delay  $t_d (\gg \delta t)$  for HE emission relative to MeV emission, the HE emission size is implied to be

$$R = 2\Gamma^2 c \frac{t_d}{1+z}. \quad (9)$$

As the MeV emission from smaller radii,  $R_{\text{MeV}} = 2\Gamma^2 c \delta t / (1+z) \ll R$ , the MeV photons in the comoving frame of the HE emission region are beamed. Let us consider an extreme case where the target photons are totally beamed in the comoving frame of the HE emission region. The optical depth is not only energy-dependent but also angle-dependent. Consider an HE photon of  $\epsilon'$  travelling with an angle  $\theta'$  relative to the target beam, then the optical depth corresponding to the distance it travels in a dynamical time is given by

$$\tau(\epsilon', \mu') = \frac{R}{2\Gamma} \int_{2m_e^2 c^4 / [\epsilon'(1-\mu')]}^{\infty} d\epsilon' \frac{dn'}{d\epsilon'} (1-\mu') \sigma(E), \quad (10)$$

where  $\mu' = \cos \theta'$ , and  $dn'/d\epsilon'$  is the energy distribution of target photons.

Consider an area element in the sphere emitting photons which lies at an angle  $\theta$  with respect to the line of sight, then in its comoving frame a photon travelling along line of sight has an angle with respect to the target photon beam of

$$\mu' = \frac{\mu - \beta_{\Gamma}}{1 - \beta_{\Gamma} \mu}. \quad (11)$$

Here  $\beta_{\Gamma} = \sqrt{\Gamma^2 - 1}/\Gamma$ . Due to Doppler effect, the photon en-

ergy in the comoving frame is related to the observed photon energy as

$$\epsilon' = \Gamma(1 - \beta_{\Gamma} \mu) \epsilon (1 + z). \quad (12)$$

Denote  $d^3 P' / d\Omega' d\epsilon' dS$  as the (comoving-frame) emitting power per unit solid angle per unit photon energy by material in per unit area of the sphere surface. This emission should be modified by  $\gamma\gamma$  attenuation factor  $e^{-\tau(\epsilon', \mu')}$ . The observed "time-averaged" flux is, then, integration over the sphere,

$$F_{\epsilon} \propto \int dS \frac{1}{\Gamma^2 (1 - \beta_{\Gamma} \mu)^2} \frac{d^3 P'}{d\Omega' d\epsilon' dS} e^{-\tau(\epsilon', \mu')}. \quad (13)$$

Assume isotropic emission power in the comoving frame, constant emissivity along the sphere, and power law dependent on photon energy, then

$$\frac{d^3 P'}{d\Omega' d\epsilon' dS} \propto \epsilon'^{-h+1}. \quad (14)$$

Using  $dS = 2\pi R^2 d\mu$  and eqs. (9), (11) and (12), we have

$$F_{\epsilon} \propto t_d^2 \Gamma^{-h+3} \epsilon^{-h+1} f(\epsilon; \Gamma), \quad (15)$$

where

$$f(\epsilon; \Gamma) = \int d\mu (1 - \beta_{\Gamma} \mu)^{-h-1} e^{-\tau(\epsilon', \mu')}. \quad (16)$$

Note that  $f(\epsilon; \Gamma)$  is the suppression factor of the primary spectrum.

It is useful to analyze this factor analytically. As shown in Appendix, for the single power-law target photon distribution,  $N(\epsilon) = N_0 \epsilon^{-s}$  and using approximation  $\sigma(E) \approx \sigma_0 E^{-2}$ , the  $f$  factor can be approximated as

$$f(\epsilon; \Gamma) = \begin{cases} 1 & \epsilon < \epsilon_{\text{br}} \\ \left( \frac{\epsilon}{\epsilon_{\text{br}}} \right)^{\frac{1}{s}-1} & \epsilon > \epsilon_{\text{br}} \end{cases}, \quad (17)$$

with the break energy at

$$\epsilon_{\text{br}} = \frac{1}{s(1+z)^2} \left[ \frac{(1+s)(2m_e^2 c^4)^s c^2 t_d}{N_0 \sigma_0 d_L^2} \right]^{\frac{1}{s-1}} \Gamma^{\frac{2(1+s)}{s-1}}. \quad (18)$$

We carry numerical calculation of  $f$  factor, and show the result in Fig 2. The analytical result is a good approximation.

Thus the spectrum is not affected until  $\epsilon > \epsilon_{\text{br}}$ , where the spectrum steepens by a factor of  $\frac{1}{s} - 1$ . Thus unlike in the case of isotropic target photons, the spectrum is not cut off exponentially but show a steepen power law. This can be easily understood- in the beam target photon case, the HE photons always can escape if they travel with a small enough angle with respect to the target beam.

The break energy is LF-dependent, thus the detection of the break in the spectrum can be used to measure the LF of GRBs.

For GRB 090510, the break energy is  $\varepsilon_{br} \approx 3$  GeV for  $\Gamma = 600$  and  $\delta t = 0.1$ s.

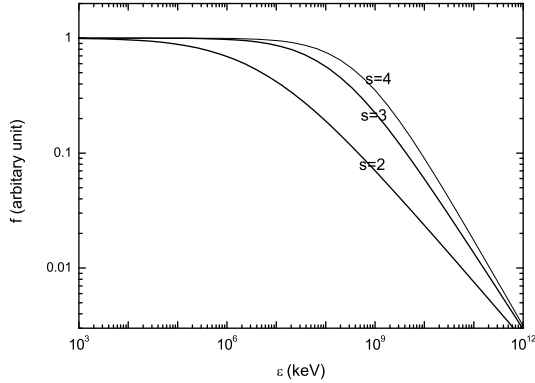


FIG. 2.— In the two-zone case the suppression factor  $f$  as function of photon energy  $\varepsilon$ . Here the target photons are assumed to be a single power law distribution. The three lines correspond to the same parameters except the target photon spectral index  $s$ , as shown in the plot.

#### 4. CASE STUDIES

In this section we study the three bright Fermi-LAT GRBs 080916C, 090510 and 090902B, and constrain their LF with assumptions of one-zone or two-zone origins.

##### 4.1. GRB 080916C

This is a bright long GRB, with a duration of  $\sim 50$ s and 145 photons detected above 100 MeV, among which 15 are beyond 1 GeV and 1 beyond 10 GeV. The redshift is quite high,  $z = 4.35$ , so that the isotropic-equivalent energy is turned out to be  $E_{iso} = 8.8 \times 10^{54}$  erg, the largest energy measured so far (Abdo et al. 2009a).

The wide energy range spectrum of this GRB is well fit by a single Band function, which may imply that all radiation is originated from one region. Indeed with one-zone assumption, the one-component spectrum favors synchrotron origin over IC emission, and the spectral slopes can be understood in the frame work of synchrotron emission model (Wang et al. 2009). Using the time interval 3.58-7.68s, and under one-zone assumption, the LF has been constrained to be  $\Gamma > 900$  by Abdo et al. (2009a). It should be noted that the constraint is variability time dependent. In this constraint  $\delta t = 2$ s is adopted from GBM light curve. However INTEGRAL also detected this GRB and show variability time in MeV range much shorter,  $\delta t < 100$  ms. With this shorter variability time, we constraint the LF to satisfy  $\Gamma > 1130$  (Fig 1).

However, the onset of  $> 100$  MeV emission is  $\sim 4$  s delayed relative to MeV emission; and in time bin "b" the bulk emission shifts toward later time as the photon energy increases, as pointed by (Abdo et al. 2009a), and the shift is 1-s scale, much longer than the variability times in MeV light curves,  $\delta t < 100$  ms, as noted by Li (2010). These temporal behaviors suggest that HE emission may have different origins and larger emission regions than the MeV one. Here we consider a simple two-zone case, where the ejecta that produce HE emission is released with a delay  $t_d = 1-4$ s relative to that produce MeV emission. We use the observed flux and spectrum to calculate the  $f$  factor to modify the original HE emission,

which is free of  $\gamma\gamma$  absorption. We consider also the time interval 3.58-7.68s, and assume the observed HE spectrum as the original one. The result is given by Fig 3, from which we see that the spectra slightly steepen at some photon energy in contrast with exponential cut-off in the one-zone case. The larger the LF, the bigger the break energy. We can see that a LF of  $\Gamma \sim 600$  can be consistent with the observed spectrum.

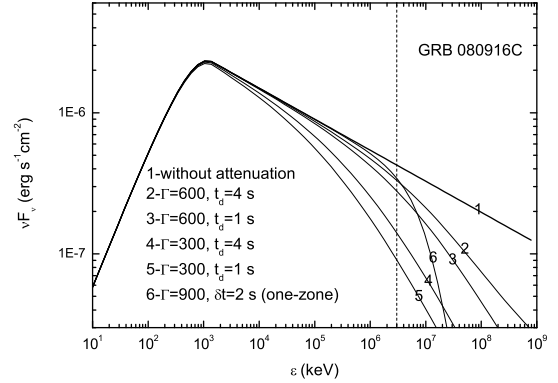


FIG. 3.— The HE suppression in the two-zone case and for GRB 080916C. Here the observed, best-fit spectrum (see Table 1) is assumed to be the original spectrum without attenuation. The vertical dashed line marks the observed highest photon energy. Also shown, for comparison, is the exponential cutoff in the one-zone case.

##### 4.2. GRB 090510

This is a short GRB with a duration of 2.1s, but very bright, with 18 photons at  $> 1$  GeV detected. Given the redshift  $z = 0.903 \pm 0.003$  and the total (0.5-1.0s) energy fluence in the 10keV-30GeV band,  $(5.02 \pm 0.26) \times 10^{-5}$  erg  $\text{cm}^{-2}$ , the total isotropic-equivalent energy release is  $(1.08 \pm 0.06) \times 10^{53}$  erg (Abdo et al. 2009b).

Using the spectrum in time interval 0.8 s-0.9 s which includes a highest energy photon of 31 GeV and can be fitted by the Band function plus a power-law component, the LF constraint in one-zone case is  $\Gamma > 1200$  (Abdo et al. 2009b). Under one-zone assumption we find that  $\Gamma > 990$  (Fig 1). The two results are in broad consistence, though our result is a little less than that of Abdo et al. (2009b), which can be due to the different definition of  $R$ . Our defined  $R$  is larger by a factor of 2.

Moreover, there are some distinct features in this GRB: the time-integrated spectrum in time interval 0.5-1.0s is best fit by two spectral components, Band-function component at low energy plus power-law component dominating HE emission; the emission above 30MeV is delayed by  $t_d = 258$  ms than those below 1 MeV. These suggest that HE may have different origin and/or emission region. Therefore we consider the simple two-zone assumption for this GRB again. We use the Band function component to calculate the optical depth and hence  $f$  factor, then we use  $f$  factor to modify the power-law component, assuming that the observed best fit spectrum as the original one without  $\gamma\gamma$  attenuation. The time delay is assumed to be  $t_d = 0.1-1$  s, because of the uncertainty. The resulted spectra are shown in Fig 4. We can find that a LF of  $\Gamma \sim 600$  can be still consistent with the spectrum.

##### 4.3. GRB 090902B

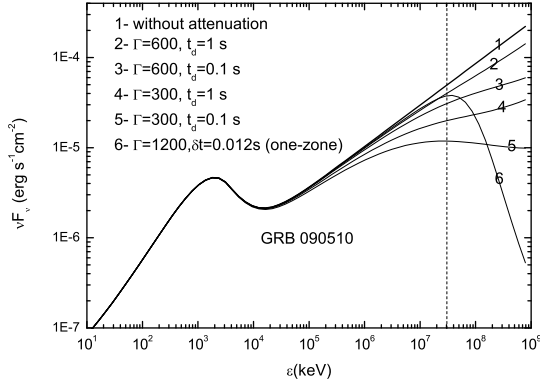


FIG. 4.— The HE suppression in the two-zone case and for GRB 090510.

With the redshift of 1.822 this long, fairly strong GRB has an isotropic-equivalent energy  $E_{\text{iso}} = 3.63 \pm 0.05 \times 10^{54}$  erg, comparable with that of the highest-energy one GRB 080916C (Abdo et al. 2009c). The duration in the energy interval 50–300 keV of Fermi (GBM) is 22 s. The highest energy photon (33.4 GeV) in this GRB is detected at 82 s after trigger, while that in the prompt phase is 11.2 GeV and in interval of 9.6–13 s. Using this time interval and one-zone assumption, Abdo et al. (2009c) constrain the LF to be  $\Gamma > 1000$  (Abdo et al. 2009c), while we get, in Fig 1,  $\Gamma > 830$ .

Similar to GRB 090510, this GRB also has a distinct spectral component fitted with a power law besides the Band function one. A peculiar characteristic of its spectrum is that its power-law component extends to lower band (<10 keV). Similar to GRB 080916C, there is an obvious delay of a few seconds in the HE onset. Look at the time bin "b" in Abdo et al. (2009c), the light curve peak seems also shift toward high energy, with a one-second delay. Then we consider again a simple two-zone case taking  $t_d = 1 - 5$  s. Similar to GRB 090510, we use the Band function component for  $f$  factor calculation, which further modify the original spectrum, assumed to be the observed spectrum. The results in Fig 5 suggest that  $\Gamma \sim 600$  can still be consistent with observations.

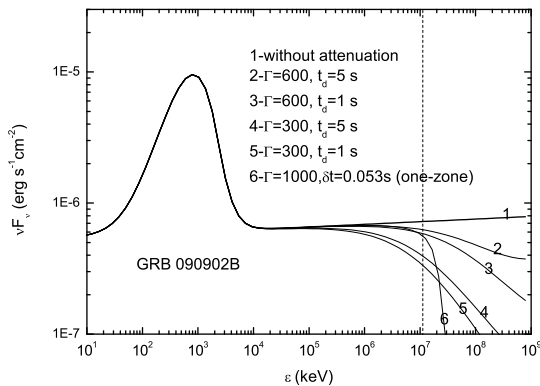


FIG. 5.— The HE suppression in the two-zone case and for GRB 090902B.

We have revisited in this work the problem of constraining the GRB LFs by the HE attenuation. Although this problem has been considered by many previous works, two concerns that have been ignored in the previous work have been emphasized here. First, we notice that in the one-zone case in order to self-consistently calculate the  $\gamma\gamma$  optical depth one needs to consider the target photons with HE spectral cutoff, other than extending to infinity. This concern is important when the LFs are below a few hundreds, or when the luminosity of GRBs are low. Second, we relax the one-zone assumption and consider a simple two-zone case where the beaming of target photons in the emission region should be taken into account. Our results show that in the two-zone case, the  $\gamma\gamma$  absorption does not lead to an abrupt spectral cutoff but a spectral steepening. If the target photon energy distribution is with a power law with photon index  $s$  then the spectral slope is changed by a factor of  $\frac{1}{s} - 1$ . This also predicts that there should be no spectral cutoff in the GRB spectra if the prompt emission is not produced in one single region. Furthermore, we take our new concerns to analyze the spectra of the three bright GRBs 080916C, 090510 and 090902B and found that in the two-zone case a LF of  $\Gamma \sim 600$  can still be consistent with the observed spectra. This relaxes the strict requirement,  $\Gamma > 10^3$ , in one-zone assumption.

We note that in the present observational situation where only tens to hundreds HE photons detected in one GRB, a slight change of the spectral slope is not easy to be identified. A single power law may still fit the HE spectral tail.

We have considered a simple two-zone case here. However the situation can be more complicated. The central engines of GRBs may naturally create variabilities in a wide range of timescales, e.g., from  $\sim 1$  ms to  $\sim 10$  s. In the framework of internal shock model, this will lead to kinetic dissipation in a wide range of radii. Even in the single-timescale case, the internal collisions will happen as the ejecta expand until the material is distributed with velocity increasing with radius. In such case we will expect multi-zone other than simple two-zone case. The time-integrated spectrum— note that the time interval with high enough photon statistic is usually much larger than the variability time— will be contributed by the multiple regions. As we can see in Figs 3–5, in the case with  $\Gamma = 300$ , the sum of the flux at the HE end can be comparable to the original flux. This means that the spectra can be consistent with a multi-zone case with the LF as low as  $\Gamma \sim 300$ .

The formation and acceleration of relativistic collimated GRB jets are open questions. In the standard "fireball" model, the thermal pressure can only accelerate the gas up to a LF  $\Gamma \lesssim 10^3$  (see, e.g., Piran 1999; Li 2010). On the other hand, simulations of magnetic-driven jets (e.g., Tchekhovskoy et al. 2009) can generate jets with the product of the LF and jet opening angle being  $\Gamma\theta_j \approx 10 - 30$ , which is consistent with pre-Fermi GRB observations. However for the bright Fermi-LAT GRBs, Cenko et al. (2010) constrained the jet opening angles by their afterglows, which, combined with the large LF,  $\Gamma > 1000$  from  $\gamma\gamma$  attenuation argument, suggests much larger values of  $\Gamma\theta_j$ . We stress here that if relaxing the one-zone assumption for GRB multi-band emission, LFs with "normal" values, say,  $\Gamma \lesssim 600$ , can still be consistent with observations. This relaxes further the theoretic problem of jet acceleration.

## 5. DISCUSSION AND CONCLUSIONS

We thank Francesco de Palma for information. XH also

thanks Z. G. Dai and X. Y. Wang for helpful discuss. This work was partly supported by the National Natural Science Foundation of China through grant 10843007 and the Foun-

dition for the Authors of National Excellent Doctoral Dissertations of China.

#### APPENDIX

##### DERIVATION OF THE SUPPRESSION FACTOR

Here we derive the suppression factor  $f$  (eq.17) in the two-zone case, assuming the target photon distribution as a single power law with  $N(\epsilon) = N_0 \epsilon^{-s}$ . In the comoving frame of the HE emission region, the target photon distribution can be given by eq (4).

The cross section of  $\gamma\gamma$  collisions in the relativistic limit ( $E \gg m_e c^2$ ) is  $\sigma(E) \approx \sigma_0 E^{-2}$ , where  $\sigma_0 = (3/8)\sigma_T(m_e c^2)^2[2\ln(2E/m_e c^2) - 1]$  weakly depend on  $E$  and can be considered as constant due to roughly a constant of  $2\ln(2E/m_e c^2) - 1$ , which is as an approximation taken as 5. With these approximations the  $\gamma\gamma$  optical depth (eq.10) can be reduced to

$$\tau = C_1 \Gamma^{-s-3} \epsilon'^{s-1} (1-\mu')^s (1+z)^{s-1}, \quad C_1 = N_0 \sigma_0 (2m_e^2 c^4)^{-s} d_L^2 (2sc^2 t_d)^{-1}. \quad (A1)$$

Using the transformations of eqs (11) and (12), the optical depth further becomes

$$\tau = C_2 \epsilon^{s-1} (1-\mu)^s (1-\beta_\Gamma \mu)^{-1}, \quad C_2 = C_1 2^s (1+z)^{2(s-1)} \Gamma^{-4}. \quad (A2)$$

As  $\theta$  increases ( $\mu$  decreases)  $\tau$  increases. Let us define the minimum  $\mu_{\min}$  where  $\tau(\epsilon, \mu_{\min}) = 1$ , then at  $\mu < \mu_{\min}$  the emission at  $\epsilon$  is significantly absorbed. Using the approximation that  $e^{-\tau} = 1$  when  $\tau < 1$  and  $e^{-\tau} = 0$  when  $\tau > 1$ , the expression for  $f$  factor is approximated by

$$f(\epsilon; \Gamma) \approx \int_{\mu_{\min}}^1 d\mu (1-\beta_\Gamma \mu)^{-h-1} \approx (1-\beta_\Gamma)^{-h-1} (1-\mu_{\min}). \quad (A3)$$

The second equality holds for  $\mu_{\min} \rightarrow 1$ .

From the definition of  $\mu_{\min}$ , we can solve out  $\mu_{\min}$ ,

$$1 - \mu_{\min} = C_2^{-\frac{1}{s}} (1-\beta_\Gamma \mu_{\min})^{\frac{1}{s}} \epsilon^{\frac{1}{s}-1} \approx C_2^{-\frac{1}{s}} (1-\beta_\Gamma)^{\frac{1}{s}} \left[ 1 + \frac{\beta_\Gamma (1-\mu_{\min})}{s(1-\beta_\Gamma)} \right] \epsilon^{\frac{1}{s}-1}, \quad (A4)$$

where the second equality in the above equation, again, holds for  $\mu_{\min} \rightarrow 1$ .

We can see that approximately,

$$1 - \mu_{\min} \propto \begin{cases} \epsilon^{\frac{1}{s}-1} & 1 - \mu_{\min} < \frac{s}{\beta_\Gamma} (1-\beta_\Gamma) \\ \text{const.} & 1 - \mu_{\min} > \frac{s}{\beta_\Gamma} (1-\beta_\Gamma) \end{cases}. \quad (A5)$$

The critical condition

$$1 - \mu_{\min} = \frac{s}{\beta_\Gamma} (1-\beta_\Gamma) \quad (A6)$$

corresponds to a "break energy"  $\epsilon_{\text{br}}$ . Substituting eq (A6) into the both sides of the first equality in eq (A4), we get

$$\epsilon_{\text{br}} = \frac{1}{s(1+z)^2} \left[ \frac{(1+s)(2m_e^2 c^4)^s c^2 t_d}{N_0 \sigma_0 d_L^2} \right]^{\frac{1}{s-1}} \Gamma^{\frac{2(1+s)}{s-1}}. \quad (A7)$$

$\epsilon > \epsilon_{\text{br}}$  corresponds to  $1 - \mu_{\min} < \frac{s}{\beta_\Gamma} (1-\beta_\Gamma)$  and  $\epsilon < \epsilon_{\text{br}}$  to  $1 - \mu_{\min} > \frac{s}{\beta_\Gamma} (1-\beta_\Gamma)$ . So we can write

$$f(\epsilon; \Gamma) \propto 1 - \mu_{\min} \propto \begin{cases} \epsilon^{\frac{1}{s}-1} & \epsilon > \epsilon_{\text{br}} \\ \text{const.} & \epsilon < \epsilon_{\text{br}} \end{cases}, \quad (A8)$$

or, after an arbitrary normalization,

$$f(\epsilon; \Gamma) = \begin{cases} 1 & \epsilon < \epsilon_{\text{br}} \\ \left( \frac{\epsilon}{\epsilon_{\text{br}}} \right)^{\frac{1}{s}-1} & \epsilon > \epsilon_{\text{br}} \end{cases}. \quad (A9)$$

#### REFERENCES

- Abdo, A. A., et al. 2009a, Science, 323, 1688  
 Abdo, A. A., et al. 2009b, Nature, 462, 331  
 Abdo, A. A., et al. 2009c, ApJ, 706, L138  
 Band, D., et al. 1993, ApJ, 413, 281  
 Baring, M. G., & Harding, A. K. 1997, ApJ, 491, 663  
 Cenko, S. B., et al. 2010, arXiv:1004.2900  
 Fenimore, E. E., Epstein, R. I., & Ho, C. 1993, A&AS, 97, 59  
 Gould R. J., & Schröder, G. P., 1967, Phys. Rev., 155, 1404  
 Greiner, J., et al. 2009, A&A, 498, 89  
 Krolik, J. H., & Pier, E. A. 1991, ApJ, 373, 277  
 Li, Z. 2010, ApJ, 709, 525  
 Li, Z., & Waxman, E. 2008, ApJ, 674, L65  
 Lithwick, Y., & Sari, R. 2001, ApJ, 555, 540  
 Piran, T. 1999, Phys. Rep., 314, 575  
 Taylor, G. B., Frail, D. A., Berger, E., & Kulkarni, S. R. 2004, ApJ, 609, L1  
 Tchekhovskoy, A., Narayan, R., & McKinney, J. C. 2009, arXiv:0909.0011  
 Wang, X.-Y., Li, Z., Dai, Z.-G., & Mészáros, P. 2009, ApJ, 698, L98  
 Waxman, E., Kulkarni, S. R., & Frail, D. A. 1998, ApJ, 497, 288  
 Woods, E., & Loeb, A. 1995, ApJ, 453, 583  
 Zhao, X. H., et al. 2010, ApJ, 708, 1357